

NEAR-INFRARED AND CO OBSERVATIONS OF W40 AND W48

MICHAEL ZEILIK II*

Department of Physics and Astronomy, University of New Mexico

AND

CHARLES J. LADA

Harvard-Smithsonian Center for Astrophysics

Received 1977 October 14; accepted 1978 January 3

ABSTRACT

Coordinated infrared observations from 1.2 to 20 μm and $^{12}\text{CO}/^{13}\text{CO}$ observations of W40 (G28.8+3.5) and W48 (G35.2-1.7) reveal that the H II regions, consisting of compact infrared components, lie on the edge of neighboring molecular clouds. Dynamical evidence supports a blister model for the development of the H II regions from their associated molecular clouds.

Subject headings: infrared: sources — interstellar: molecules — nebulae: individual

I. INTRODUCTION

Advances in millimeter and infrared detection have prompted a deluge of observations of H II region/molecular cloud complexes in the Galaxy. In these regions (such as M17, M8, M42, and W3), compact infrared sources—indicative of recent formation of massive stars—lie in physical association with H II regions and molecular clouds. Observations in such cases support a blister model (Israel 1976) for the evolution of H II regions at the surfaces of molecular clouds. As an H II region expands, one side dissipates into the interstellar medium, while the other pushes into the molecular cloud and generates a shock front. Elmegreen and Lada (1977) have proposed that such shock fronts driving into a molecular cloud can trigger star formation of a small cluster of OB stars.

* Visiting Astronomer, Kitt Peak National Observatory, which is operated by the Association of Universities for Research in Astronomy, Inc., under contract AST 74-04129 with the National Science Foundation.

This model pictures massive star formation as taking place at the *interfaces* of H II regions and molecular clouds.

We have coordinated near-infrared (1.2–20 μm) and millimeter observations of W40 (G28.8+3.5) and W48 (G35.2-1.7). These observations support a blister model for the development of these H II regions from their associated molecular clouds.

II. OBSERVATIONS

Goss and Shaver (1970) and Shaver and Goss (1970a) observed W40 and W48 at 5 GHz and 408 MHz; we use their galactic designations of G28.8+3.5 and G35.2-1.7 (Table 1). Later, Felli, Tofani, and D'Addario (1974) detected fine structure in W48 at 10.7 GHz; their observations indicated two compact components.

a) Infrared

These radio observations prompted Zeilik (1975) to survey W40 and W48 to search for infrared emission,

TABLE 1
 INFRARED AND RADIO POSITIONS

SOURCE	FREQUENCY OR WAVELENGTH	POSITION (1950)		REFERENCE
		R.A.	Decl.	
G28.8+3.5.....	408 MHz	18 ^h 28 ^m 49 ^s 0	-02°07'35"	Shaver and Goss (1970a)
G28.8+3.5.....	5 GHz	18 28 51	-02 07 29	Reifenstein <i>et al.</i> (1970)
W40/IRS 1.....	2.2 μm	18 28 51.7	-02 07 33	This work
W40/IRS 2.....	2.2 μm	18 28 47.7	-02 07 41	This work
W40/IRS 3.....	2.2 μm	18 28 47.6	-02 06 19	This work
W40/ ^{12}CO peak.....	115 GHz	18 28 39.7	-02 08 58	This work
G35.2-1.8.....	408 MHz	18 59 15.3	+01 08 14	Shaver and Goss (1970a)
W48.....	15.4 GHz	18 59 14.5	+01 08 16	Schraml and Mezger (1969)
G35.2-1.7.....	5 GHz	18 59 15	+01 09 04	Reifenstein <i>et al.</i> (1970)
W48/IRS 1.....	2.2 μm	18 59 14.7	+01 08 53	This work
W48/IRS 2.....	2.2 μm	18 59 12.2	+01 08 20	This work
W48.....	3.4-33 μm	18 59 14.2	+01 08 41	Dyck and Simon (1977)
W48/ ^{12}CO peak.....	115 GHz	18 59 08	+01 09 00	This work

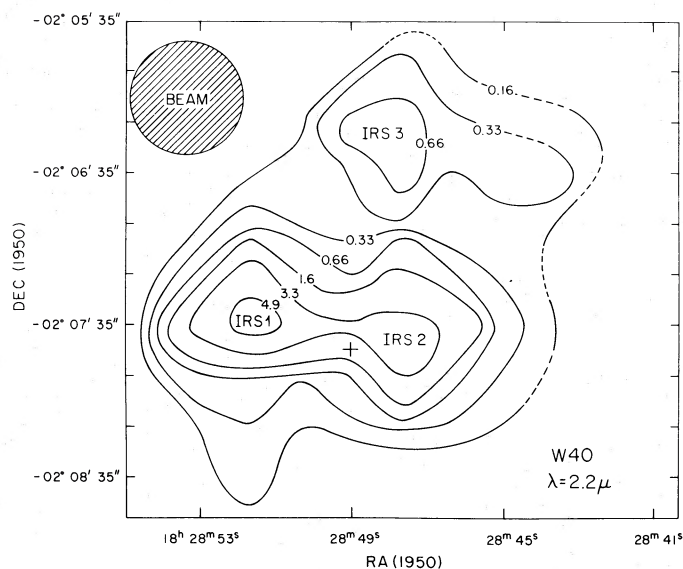


FIG. 1.—A $2.2 \mu\text{m}$ intensity map of W40. The area out to last contour was sampled at half-beamwidth intervals with a $44''$ beam. Beam separation was $240''$ in declination. The cross indicates the 408 MHz position of Shaver and Goss (1970a).

which was found close to the peak radio positions of Shaver and Goss (1970a). The initial observations were made on the 1.3 m telescope at Kitt Peak National Observatory¹ with the KPNO bolometer ($11''$ beam) and the SAO bolometer ($18''$ beam). The negative and positive beams were separated in declination by $100''$. Later observations, done mostly during the day, used the KPNO InSb system ("Otto") with a variable beam from $6''$ to $63''$. Primary standard stars were α Boo, α Sco, and α Lyr. The scale of Low and Rieke (1974) provided the absolute calibrations for the zeroth-magnitude flux densities.

i) W40

Figure 1 presents the brightness distribution of $2.2 \mu\text{m}$ emission from W40 with a $44''$ beam mapped at half-beamwidth intervals. Note the appearance of three peaks; the strongest—IRS 1—lies close to the radio peaks of Shaver and Goss (1970a) and Felli, Tofani, and D'Addario (1974). The integrated flux density of the mapped area is $11 \pm 1 \text{ Jy}$ at $2.2 \mu\text{m}$.

Using the 36.5 m Haystack² antenna at 15.4 GHz, Zeilik obtained a flux density of $5.1 \pm 0.5 \text{ Jy}$ (compared with DR 21) for a $2'$ beam centered on a position about halfway between IRS 1 and IRS 2. The formulae of Willner, Becklin, and Visvanathan (1972) predict a $2.2 \mu\text{m}$ flux density of 1.8 Jy from the ionized gas alone from this 15 GHz flux density. So a substantial amount of the $2.2 \mu\text{m}$ emission arises from dust in the H II region.

¹ Kitt Peak National Observatory is operated by AURA, Inc. under contract with the National Science Foundation.

² The Haystack Observatory of the Northeast Observatory Corporation is supported in part by the National Science Foundation.

Figure 2 shows spectral power distributions of IRS 1–3 for various beam sizes. Note that IRS 1 has a steep rise to $20 \mu\text{m}$ typical for dusty, compact H II regions. While not observed beyond $5 \mu\text{m}$, both IRS 2 and IRS 3 appear to be rising in a similar manner.

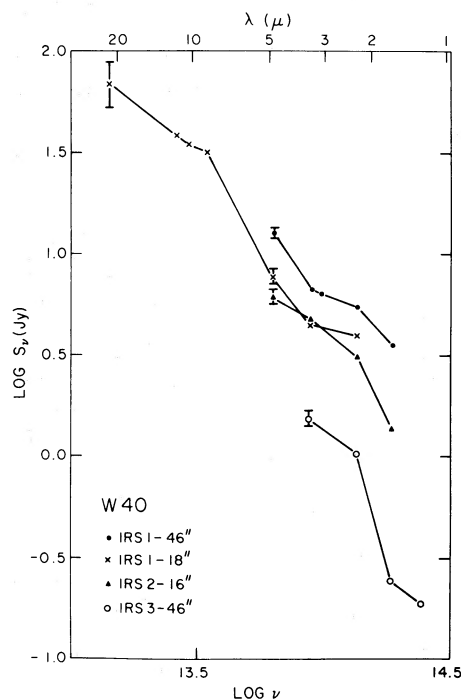


FIG. 2.—Spectral brightness distributions for IRS 1, 2, and 3 in W40. Note that IRS 1 was observed with two different beam sizes ($18''$ and $46''$).

Shaver and Goss (1970*b*) give a distance to W40 of only 0.7 kpc. (At this distance, the infrared sources have sizes on the order of tenths of a parsec.) This proximity is suggested by the fact that optical emission is partially visible at W40's position on the Palomar Observatory Sky Survey plates. So the extinction toward W40 is probably not substantial, and we ignore it in the calculation of the intrinsic 2–20 μm luminosity. (This procedure underestimates the 2–20 μm luminosity.) We assume that the 63" to 16" ratio at 2.2 μm for IRS 1 holds at all wavelengths. Then, at 0.7 kpc, $L_{2-20\mu\text{m}}$ (IRS 1) = 14×10^{28} watts or $3.6 \times 10^2 L_{\odot}$. If IRS 2 and IRS 3 have the same spectral index to 20 μm as IRS 1, then $L_{2-20\mu\text{m}}$ (total) $\approx 7 \times 10^2 L_{\odot}$, and $L_{2-20\mu\text{m}}/L_{\alpha} \approx 1.4$. The fact that this ratio is greater than 1 implies some stellar-continuum heating of the grains in the H II region, as expected from a two-component dust model (Natta and Panagia 1976; Zeilik 1975, 1977).

Olthof (1974) reported 81 μm and 140 μm flux densities of $1.0 \times 10^{-21} \text{ W m}^{-2} \text{ Hz}^{-1}$ and $8.6 \times 10^{-22} \text{ W m}^{-2} \text{ Hz}^{-1}$ for a far-infrared source identified with W40 measured with a 0.5 beam. These results give $L_{20-140\mu\text{m}} = 2.8 \times 10^4 L_{\odot}$, about 40 times greater than the $L_{2-20\mu\text{m}}$.

ii) W48

Similar infrared observations were performed on W48. Figure 3 shows a 3.5 μm map of the region and indicates two close, compact infrared components (IRS 1 and IRS 2). Only IRS 1, the stronger, was observed from 1.2 to 21 μm (Fig. 4). The rise in the spectrum is steeper than that for any component of W40.

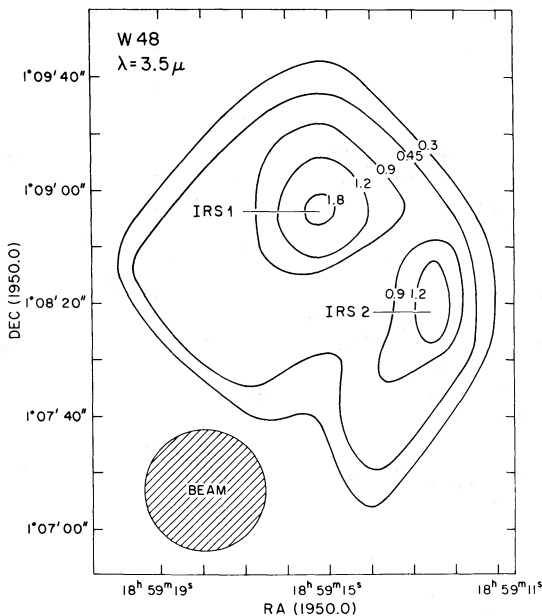


FIG. 3.—A 3.5 μm intensity map of W48. The area out to last contour was sampled at half-beamwidth intervals with a 44" beam. Beam separation was 240" in declination.

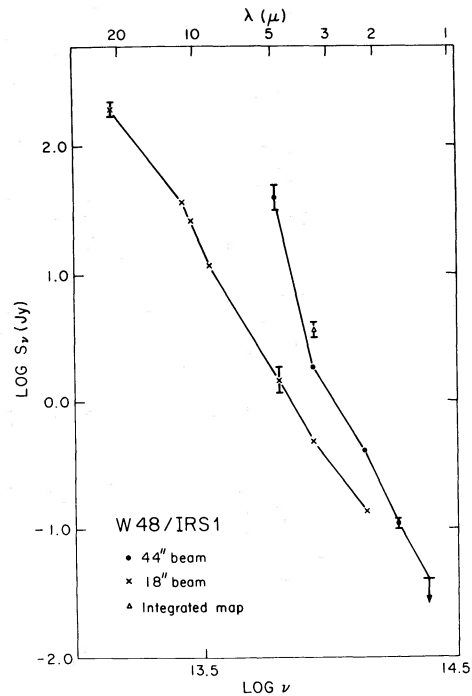


FIG. 4.—Spectral power distribution of W48/IRS 1 with a 18" and 44" beam. Error bars are statistical only. The 5 μm observation with the 44" beam was made on a night with high extinction at 5 μm through a large air mass; actual uncertainty in this datum is estimated to be about 50%.

Zeilik used the Haystack antenna at 15.4 GHz to measure a flux density of $12 \pm 1.2 \text{ Jy}$ centered on IRS 1. From this, the formulae of Willner, Becklin, and Visvanathan (1972) predict a 3.5 μm flux density of 3.9 Jy. Integrating the 3.5 μm map, we find a total flux density of $3.7 \pm 0.4 \text{ Jy}$. So the source does not appear to have an excess at 3.5 μm . However, W48 does not appear on the POSS plates; this indicates substantial visual extinction, implying that the infrared extinction may be large enough to lower the actual value at 3.5 μm to appear without an excess. If we compare the ratio at 1.67 μm and 2.2 μm predicted from the radio observations with the observed one and apply van de Hulst curve number 15 (Johnson 1968), we find that $A_v \approx 14$ —a value consistent with the source not appearing on the POSS plates. With this conservative value for the visual extinction, and assuming that the integrated map to 18" beam ratio at 3.5 μm holds at all wavelengths, we calculate that $L_{2-20\mu\text{m}} = 5.9 \times 10^4 L_{\odot}$, if W48 is at 3.2–3.4 kpc (Bridle and Kesteven 1972; Reifenstein *et al.* 1970). Then $L_{2-20\mu\text{m}}/L_{\alpha} = 1.3$.

Dyck and Simon (1977) reports a value of $L_{2-20\mu\text{m}} \approx 0.4 \times 10^4 L_{\odot}$ for W48 at 3.4 kpc. This luminosity is lower than ours because Dyck and Simon measured only the peak flux density in a 13.5 beam. They noted that the infrared emission from W48 continues to rise to 33 μm , and scaling up their $L_{2-33\mu\text{m}}$ luminosity by 10, we have $L_{2-33\mu\text{m}} \approx 10^5 L_{\odot}$, and $L_{2-33\mu\text{m}}/L_{\alpha} \approx 2.3$, as expected from the models of Natta and

Panagia (1976) and Zeilik (1977), where both $L\alpha$ and stellar continuum photons heat the dust.

b) Carbon Monoxide Observations

To see if the near-infrared sources in W40 and 48 are associated with molecular cloud features, we observed $J = 1-0$ transitions of ^{12}CO and ^{13}CO in the vicinity of both sources. The observations were made in 1976 February with the 5 m millimeter wave telescope at McDonald Observatory.³ Lada, Dickinson, and Penfield (1974) have described the basic equipment and observing procedure for this antenna. The ^{12}CO antenna temperatures were corrected for atmospheric absorption and instrumental effects following the method of Davis and Vanden Bout (1973).

i) W40

We mapped ^{12}CO emission in an area about $12' \times 18'$ around W40/IRS 1. Figure 5 shows the results of these observations displayed as a contour map of peak ^{12}CO emission. The positions of the three infrared sources are represented by a box approximately the same size as the field mapped in Figure 1. A strong peak of CO emission ($T_b \sim 31$ K; $V_{\text{LSR}} \sim 4.5$ km s $^{-1}$) lies displaced about $1.5'$ southwest from the infrared sources. This peak appears to be within an elongated plateau of enhanced CO emission ($T_b \sim 15$ K), which extend in a north-south direction west of the infrared sources.

We have measured emission from ^{13}CO at the peak position in order to make an estimate of the CO column density in this source. The observed ^{13}CO

³ The Millimeter Wave Observatory is operated by the Electrical Engineering Research Laboratory of the University of Texas, with support from the National Aeronautics and Space Administration, the National Science Foundation, and McDonald Observatory.

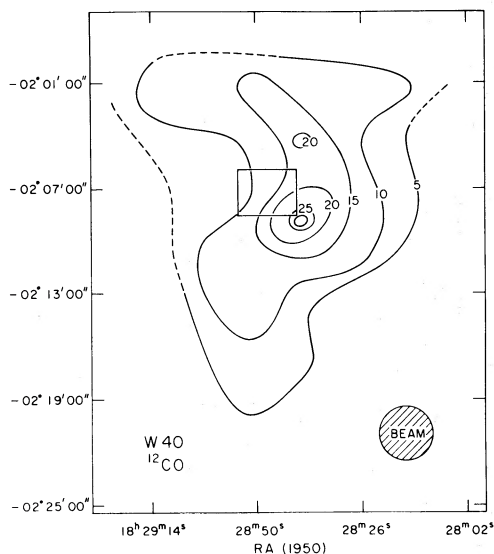


FIG. 5.— ^{12}CO intensity map of the W40 region. The box indicates the area shown in Fig. 1.

line parameters of $T_b = 9.3$ K and $\Delta V = 2.2$ km s $^{-1}$ result in a column density of $N(^{13}\text{CO}) = 5.6 \times 10^{16}$ cm $^{-2}$. We have used the equation $N(^{13}\text{CO}) = 2.85 \times 10^{14} \tau^{13} \Delta V^{13} (T_{ex} + 0.91) / [1 - \exp(-5.29/T_{ex})]$ to calculate the ^{13}CO abundances. The observed column density toward W40 is typical of that observed toward most giant molecular clouds associated with H II regions.

The local standard of rest (LSR) radial velocity of the ^{12}CO emission at the peak position is about 4.5 km s $^{-1}$. Reifenstein *et al.* (1970) and Pankonin, Thomasson, and Barsuhn (1977) find a velocity of 0.7 km s $^{-1}$ for the H109 and H166 α recombination lines from the W40 H II region. The velocity of the C166 α line is 6.4 ± 1.5 km s $^{-1}$. The difference between the hydrogen recombination line and CO radial velocities of about 4 km s $^{-1}$ is not unusual for the majority of molecular cloud/H II region associations (Wilson *et al.* 1974) and, as we will show later, can be explained in terms of a blister model (Israel 1976).

ii) W48

Results of our ^{12}CO observations for W48 are shown in a contour map of peak CO emission in Figure 6. The observed lines toward W48 were unusually broad (8–10 km s $^{-1}$) and so occupied a significant fraction of our bandpass (26 km s $^{-1}$). Consequently, determination of accurate temperatures through this region is somewhat uncertain, and observations with more spectral coverage should be performed in the future to confirm our results. Two peaks in CO emission are evident. The northern peak appears to coincide with an H $_2$ O/OH maser source observed by Turner and Rubin (1971). The southern peak is near, but not coincident with, the W48 infrared sources. Observations of ^{13}CO in the western portion of the cloud resulted in a column density determination of $N(^{13}\text{CO}) = 5.5 \times 10^{16}$ cm $^{-3}$. We estimate an LSR velocity of about 41 km s $^{-1}$ for this

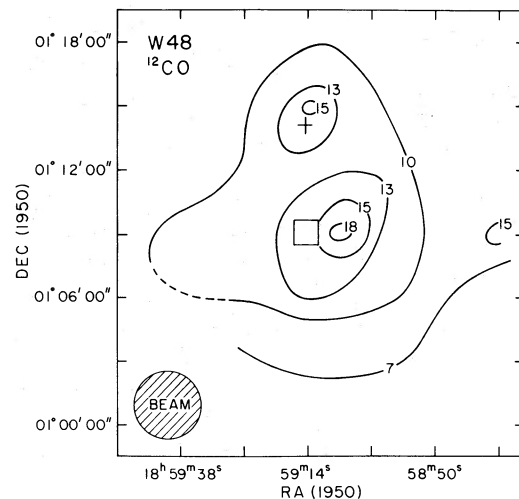


FIG. 6.— ^{12}CO map of the W48 region. The box indicates the area shown in Fig. 3.

cloud, but because of the large line width this estimate is somewhat uncertain. The hydrogen recombination-line velocities of 45.2 km s^{-1} for H158 α and 44.1 km s^{-1} for H166 α are slightly higher than the CO estimate, while the corresponding carbon-line velocities of 42.9 and 42.4 km s^{-1} are almost the same as the CO lines (Pankonin, Thomasson, and Barsuhn 1977).

III. DISCUSSION AND CONCLUSIONS

Our observations of W40 and W48 provide two clues pertinent to understanding the interrelationship of the molecular clouds and H II regions in these sources. First, the measured velocities of hydrogen recombination lines *differ* from those of CO in both sources. The difference $V(\text{H II}) - V(\text{CO})$ is roughly 4 km s^{-1} for each region. In W40 this difference is negative, and in W48 it is positive. For both, the velocities of carbon recombination lines fall close to those of CO.

We interpret these data by a hot, blister model, whose general applicability has been demonstrated by Israel (1976). In this model, H II regions expand away from the surface of the molecular clouds, and the observed velocity difference between the ionized and molecular gas depends on the relative line-of-sight orientation of the neutral and ionized components. This difference $[V(\text{H II}) - V(\text{CO})]$ is negative, zero, or positive when the H II region is in front, at the side, or behind the molecular cloud. Our observations of W40 imply that, along the line of sight, the H II region is at the front edge of the molecular cloud. That this H II region is faintly visible on the Palomar Observatory Sky Survey (classified as S64) agrees with this type of geometry. In contrast, the positive velocity difference for W48 implies that the H II region is on the far side of its associated molecular cloud. Its absence on the POSS and the large value of extinction inferred for this source (see § IIbii) is consistent with such a line-of-sight geometry.

The closer agreement of the carbon recombination-line velocities with that of CO rather than that of H II is understandable if the carbon-emitting regions of primarily neutral material lie at the edge of the molecular cloud, near its interface with the H II region (cf. Zuckerman and Ball 1974).

Our second important result is that the infrared sources are *displaced* from the peaks of CO emission. (The displacement projected on the sky is about 0.5 pc for W40 and 1.5 pc for W48.) The positions of the infrared sources in both do correspond to the peaks in radio continuum emission. This coincidence implies that the infrared emission comes from the H II regions and not from sources embedded in the molecular

clouds. It also indicates that the positions of the H II regions along the line of sight are not "directly" either in front (W40) or behind (W48) their respective molecular clouds but are located partially to the side of the clouds. The separation of emission peaks from H II regions and molecular clouds supports the blister model (Israel 1976).

The best test of the blister model for a given region is to determine whether the H II regions are actually in physical contact with the molecular clouds, a fact usually assumed but not easily demonstrated. Presence of optical bright rims, steep gradients in radio continuum emission, and CO contour maps indicate a physical interaction between a molecular cloud and an H II region (e.g., Lada *et al.* 1976; Lada and Black 1976). Such an interaction is suggested in high-resolution continuum maps of W40 at 408 MHz (Shaver and Goss 1970a). This map shows an indentation of the radio continuum contours near the region of peak molecular emission. This deviation from circular symmetry in the continuum map suggests that the H II region is in contact with the molecular cloud in that region. Higher-resolution continuum maps would probably show steep gradients in continuum emission at this interface.

Our CO and infrared observations of W40 and W48 indicate that these H II regions lie at the edges of molecular clouds, in support of a blister model. Recently, Lada (1976) and Elmegreen and Lada (1977) proposed that ionization fronts at the H II region/molecular cloud interface drive shock fronts into molecular clouds and trigger further star formation in a sequential process. Applying this model to W40 and W48, we would expect to find newly formed stars at the interfaces and/or at the positions of the CO peaks. These peak positions were searched by Zeilik at KPNO at $2.2 \mu\text{m}$ with a $44''$ beam. No emission at a 3σ upper limit was found in boxes $2''$ around the four CO peaks. This lack probably indicates that, if young stars are present, they have not yet heated their surroundings sufficiently to be detected as near-infrared sources. In contrast, the H₂O/OH maser at the north W48 peak may result from shock-driven star formation.

Searches for far-infrared and $20 \mu\text{m}$ sources and H₂O emission should be carried out at the CO peaks and along the H II region/molecular interfaces to help determine if a sequential star formation model applies to W40 and W48.

We are grateful to Bruce Elmegreen and Dale Dickinson for assistance with the CO observations. M. Zeilik was supported in part by the Research Allocations Committee of the University of New Mexico.

REFERENCES

- Bridle, A. H., and Kesteven, M. J. L. 1972, *A.J.*, **77**, 207.
 Davis, J., and Vanden Bout P. 1973, *Ap. Letters*, **15**, 43.
 Dyck, H. M., and Simon, T. 1977, *Ap. J.*, **211**, 421.
 Elmegreen, B. G., and Lada, C. J. 1977, *Ap. J.*, **214**, 725.
 Felli, M., Tofani, G., and D'Addario, L. R. 1974, *Astr. Ap.*, **31**, 431.
 Goss, W. M., and Shaver, P. A. 1970, *Australian J. Phys. Ap. Suppl.*, **14**, 1.
 Israel, F. P. 1976, Ph.D. thesis, Sterrewacht, Leiden.
 Johnson, H. L. 1968, in *Nebulae and Interstellar Matter*, ed. B. M. Middlehurst and L. H. Allen (Chicago: University of Chicago Press), p. 167.

- Lada, C. J. 1976, *Ap. J. Suppl.*, **32**, 603.
 Lada, C. J., and Black, J. J. 1976, *Ap. J. (Letters)*, **203**, L75.
 Lada, C. J., Dickinson, D. F., Gottlieb, C. A., and Wright, E. L. 1976, *Ap. J.*, **207**, 113.
 Lada, C. J., Dickinson, D. F., and Penfield, H. 1974, *Ap. J. (Letters)*, **189**, L35.
 Low, F. J., and Rieke, G. 1974, in *Methods of Experimental Physics*, v. **12**, part A, ed. N. Carleton (New York: Academic Press) p. 415.
 Natta, A., and Panagia, N. 1976, *Astr. Ap.*, **50**, 191.
 Olthof, H. 1974, *Astr. Ap.*, **33**, 471.
 Pankonin, V., Thomasson, P., and Barsuhn, J. 1977, *Astr. Ap.*, **54**, 335.
 Reifenstein, E. C., III, Wilson, T. L., Burke, B. F., Mezger, P. G., and Altenhoff, W. J. 1970, *Astr. Ap.*, **4**, 357.
 Schraml, J., and Mezger, P. G. 1969, *Ap. J.*, **156**, 269.
 Shaver, P. A., and Goss, W. M. 1970a, *Australian J. Phys. Ap. Suppl.*, **14**, 77.
 ———. 1970b, *Australian J. Phys. Ap. Suppl.*, **14**, 133.
 Turner, B. E., and Rubin, R. H. 1971, *Ap. J. (Letters)*, **170**, L113.
 Willner, S. P., Becklin, E. E., and Visvanathan, N. 1972, *Ap. J.*, **175**, 699.
 Wilson, W. J., Schwartz, P. R., Epstein, E. E., Johnson, W. A., Etcheverry, R. D., Mori, T. T., Berry, G. G., and Dyson, G. B. 1974, *Ap. J.*, **191**, 357.
 Zeilik, M., II. 1975, Ph.D. thesis, Harvard University.
 ———. 1977, *Ap. J.*, **213**, 58.
 Zuckerman, B., and Ball, J. 1974, *Ap. J.*, **190**, 35.

C. J. LADA: Center for Astrophysics, 60 Garden Street, Cambridge, MA 02138

M. ZEILIK II: Department of Physics and Astronomy, University of New Mexico, 800 Yale Boulevard NE, Albuquerque, NM 87131